THE JOURNAL OF PHYSICAL CHEMISTRY Letters

Letter

pubs.acs.org/JPCL

$PtZnH_5^-$, A σ-Aromatic Cluster

Xinxing Zhang,[†] Gaoxiang Liu,[†] Gerd Ganteför,[†] Kit H. Bowen,*[,†] and Anastassia N. Alexandrova*[,‡,§]

[†]Department of Chemistry and Materials Science, Johns Hopkins University, Baltimore, Maryland 21218, United States

[‡]Department of Chemistry and Biochemistry, University of California, Los Angeles, Los Angeles, California 90095-1569, United States

[§]California NanoSystems Institute, 570 Westwood Plaza, Building 114, Los Angeles, California 90095, United States

Supporting Information

ABSTRACT: We report a joint photoelectron spectroscopic and theoretical study of the $PtZnH_5^-$ cluster anion. This cluster exhibited an unprecedented planar pentagonal coordination for Pt and an unusual stability and high intensity in the mass spectrum. Both are due to the σ-aromaticity found in the H_5-cycle supported by the 5d orbitals on the Pt atom. σ-Aromaticity in all-H systems has been predicted in the past but never found in experimentally observed species. Besides fundamental importance, mixed transition-metal hydrides can be found as intermediates in catalytic processes, and thus, the unexpected stability facilitated by σ-aromaticity can be appreciated also in practical applications.

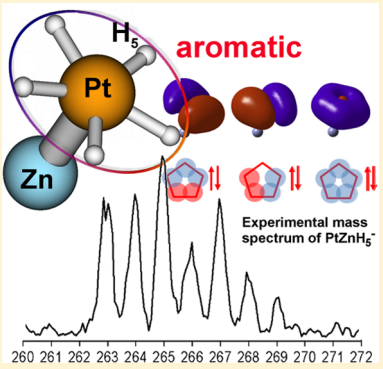

SECTION: Molecular Structure, Quantum Chemistry, and General Theory

Aromaticity, one of the most significant concepts in modern chemistry, continues to gain appreciation as it is one of the stabilizing chemical bonding effects that leads to remarkable symmetries and stabilities of clusters and molecules.[1−16] Many all-metal clusters were reported to exhibit multiple types of aromaticity, including σ-, π-, and δ-type or a combination of these three types. σ-Aromaticity in particular has been a concept first subjected to debates and prosecution and then accepted and widely explored. The simplest systems in which σ-aromaticity can be found are clusters of H, where the bonding overlap of the 1s atomic orbitals (AOs) on atoms gives rise to this phenomenon. The peculiar example of this sort is the H_3^+ cluster, a highly abundant species in the interstellar space. Species decorated with multiple hydrides also occur in heterogeneous catalysis, and there, every bit of stability (whether or not due to aromaticity) counts toward or against the kinetics of the catalytic processes. Intriguingly, in 2003, Tsipis et al. theoretically predicted the existence of aromatic metal hydride clusters M_nH_n(M = Cu, Ag, Au; n = 3−6);[17−20] however, their experimental evidence is still absent. It would be exciting to see if the simplest possible type of aromaticity and antiaromaticity (σ-type) could be present in metal hydrides and govern their stability, in particular, if one day this could be explored in catalytic processes.

In this work, we study mixed Pt−Zn hydrides at the subnano scale. The Pt−Zn bimetallic systems are used as catalysts for various reactions, such as hydrogenation/dehydrogenation and fuel cell oxidation.[21−26] Doping precious metal catalysts in general is an amendable strategy for manipulating and tuning the electronic structure and thus properties of the catalyst and potentially reducing the cost. However, the research is still within the nanoregime, and subnano bimetallic Pt−Zn clusters containing only several atoms have not been studied but pose a great interest in view of the observation that small clusters are actually the sites where the majority of catalytic processes occur.[27−29] Hydrides of these small clusters are thus of interest.

We present a combined experimental and theoretical study of a σ-aromatic cluster, $PtZnH_5^-$, and also of $PtZnH_3^-$ and $PtZnH_4^-$. These anionic hydrides are generated in the gas phase and investigated using negative ion photoelectron spectroscopy (PES). The experimental photoelectron spectra are compared with theoretical predictions for the found global minimum structures. $PtZnH_5^-$ is found to have an unusual structure, high stability manifested in the abundance in the mass spectrum, and σ-aromaticity.

Experimental Results. The mass spectrum of the $PtZnH_5^-$ cluster anion is presented in Figure 1A. One can observe several major isotopic peaks ranging from 261 to 271. In order to make sure that the spectrum has no impurities from other hydrides, that is, $PtZnH_n^-$, we plotted the simulated isotopic distribution of $PtZnH_5^-$ in Figure 1B. One can observe that both spectra match very well not only in distribution but also in relative intensity. This phenomenon is uncommon for mass spectrometric study of metal hydrides; typically, there are different numbers of hydrogen atoms attached to the metal atom. Thus,

Received: February 13, 2014
Accepted: April 16, 2014
Published: April 16, 2014

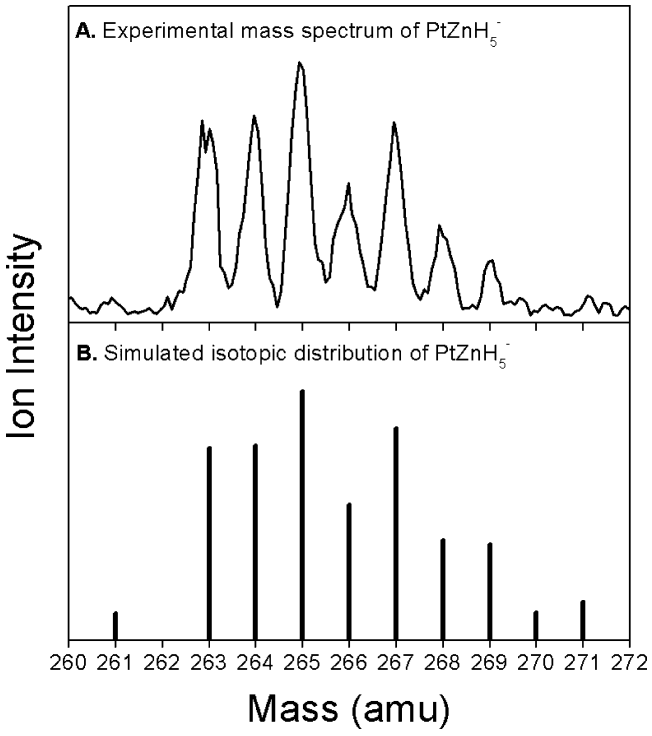

Figure 1. Experimental (A) and simulated (B) mass spectra of $PtZnH_5^-$.

the triumph of $PtZnH_5^-$ from the $PtZnH_n^-$ series indicates its special stability.

Figure 2 presents the photoelectron spectrum of $PtZnH_5^-$ taken with a 355 nm (3.496 eV) laser. We took spectra from all

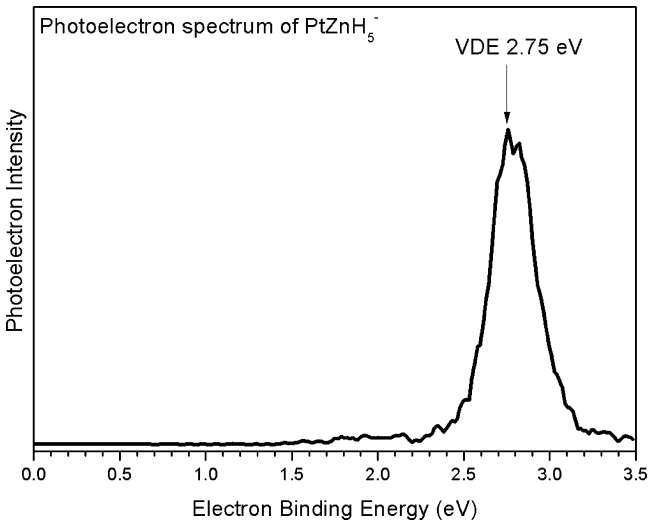

Figure 2. Photoelectron spectrum of $PtZnH_5^-$ recorded using 355 nm (3.496 eV) photons.

of the isotopic peaks, and all of them were identical, which is another confirmation that there is no contamination in the mass spectrum. One observes a major EBE band ranging from 2.4 to 3.2 eV and peaked at 2.75 eV, with the resolution being better than 50 meV. The electron binding energy (EBE) value corresponding to the intensity maximum in the observed band is its vertical detachment energy (VDE), the transition energy at which the Franck–Condon overlap between the wave functions of the anion and its neutral counterpart is maximal. The adiabatic electron affinity (EA) is the energy difference between the lowest energy vibronic state of the anion and the lowest energy vibronic state of its neutral counterpart. We have estimated the EA of $PtZnH_5$ to be 2.5 eV by extrapolating the low EBE side, with the corresponding EBE value there being taken as the EA.

Cluster Structures. Figure 3 shows the found global minima of considered clusters, $PtZnH_3^-$, $PtZnH_4^-$, and $PtZnH_5^-$; for

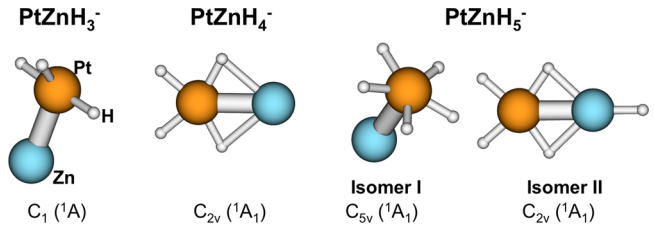

Figure 3. Calculated global minima of $PtZnH_{3,4}^-$ and two competing isomers of $PtZnH_5^-$.

$PtZnH_5^-$, we show the global minimum and the second competing isomer. All clusters bind atomic H, which indicates that they would likely dissociate H_2, should it bind to them as a molecule, for example, in a catalytic process. Indeed, Pt is a typical catalyst for dehydrogenation, in the form of extended surfaces, nanoparticles, and nanoislands, even though catalysis of really small clusters was hardly ever explored. For $PtZnH_3^-$, the global minimum is a C_1 (^{1}A) structure, with all three H atoms bound to the Pt atom. For $PtZnH_4^-$, it is the C_{2v} ($^1A_1$) structure, with two of the four H atoms bridging between Pt and Zn and the remaining two bound to Pt. For $PtZnH_5^-$, there are two isomers relatively close in energy. Most theoretical methods predict isomer II (C_{2v} ($^1A_1$)) to be more stable by ~4 kcal/mol. One exception is the CASSCF(12,12) method, which predicts isomer I (C_{5v} ($^1A_1$)) to be more stable. Considering the expected error in the performance of the ab initio method in use, it is fair to say that these two isomers are isoenergetic. Calculated properties of both isomers are shown in the Supporting Information.

Theoretical Interpretation of the Photoelectron Spectrum of $PtZnH_5^-$. In this work, we focus on $PtZnH_5^-$ because of its unusually high abundance in the mass spectrum as compared to the two lighter hydrides. We expect it to exhibit unusual structure and bonding characteristics. Table 1 shows calculated photoelectron spectra of the two isomers of $PtZnH_5^-$. The agreement across different theoretical methods is apparent. The simulated spectrum of isomer II does not agree with the experiment, with VDE_1, being ~1 eV off, and that rules out the possibility of the isomer II being observed in the experiment. On the other hand, the theoretical spectrum of isomer I is in close agreement with the experiment. All experimental features are successfully assigned to single-electron processes of electron detachment from the valence molecular orbitals (MOs) shown in Figure 4A. The fact that isomer I is predicted to be less stable but is the one observed experimentally indicates either the inadequate performance of theoretical methods or the kinetic stabilization of the metastable isomer I in the beam. The predicted adiabatic detachment energy (ADE) is close to the VDE (Table 1), and in the experiment, the observed EA, 2.5 eV, and the theoretical ADE are effectively the same quantities in this case. The electron detachment from the completely symmetric HOMO of the cluster leads to a small geometric

dx.doi.org/10.1021/jz500322n | J. Phys. Chem. Lett. 2014, 5, 1596–1601

Table 1. Calculated Photoelectron Spectra of $PtZnH_5^-$ Isomers I and II, in eV

peak	expl. VDE/EA	MO	resultant e-configuration	TD-UPBEPBE,[a] VDE/ADE	TD-UPBEPBE,[b] VDE/ADE	CCSD(T)
Isomer I						
X	2.75/2.5	HOMO	$...2a_1^2 2e_2^4 3a_1^2 2e_1^4 3e_1^4 4a_1^1$	2.71/2.58	2.70/2.51	2.50[c]
		HOMO−1	$...2a_1^2 2e_2^4 3a_1^2 2e_1^4 3e_1^3 4a_1^2$	4.48[d]	4.50[d]	
		HOMO−2	$...2a_1^2 2e_2^4 3a_1^2 2e_1^3 3e_1^4 4a_1^2$	4.93[d]	4.92[d]	
		HOMO−3	$...2a_1^2 2e_2^4 3a_1^1 2e_1^4 3e_1^4 4a_1^2$	5.83	5.91	
		HOMO−4	$...2a_1^2 2e_2^3 3a_1^2 2e_1^4 3e_1^4 4a_1^2$	7.12[d]	7.13[d]	
Isomer II						
X	2.75/2.5	HOMO	$...5a_1^2 6a_1^2 3b_2^2 2b_1^2 2a_2^2 7a_1^1$	3.68	3.65	3.84[c]
		HOMO−1	$...5a_1^2 6a_1^2 3b_2^2 2b_1^2 2a_2^1 7a_1^2$	3.97	4.02	
		HOMO−2	$...5a_1^2 6a_1^2 3b_2^2 2b_1^1 2a_2^2 7a_1^2$	4.17	4.19	
		HOMO−3	$...5a_1^2 6a_1^2 3b_2^1 2b_1^2 2a_2^2 7a_1^2$	4.46	4.67	
		HOMO−4	$...5a_1^2 6a_1^1 3b_2^2 2b_1^2 2a_2^2 7a_1^2$	4.70	5.17	

[a]The aug-cc-pvTZ-pp basis set was used. [b]The 6-311++G** basis was used for Zn and H, and LANL2DZ(+f) was used for Pt. [c]At the geometry of the anion optimized using MP2/aug-cc-pvTZ-pp. [d]Indicates doubly degenerate features.

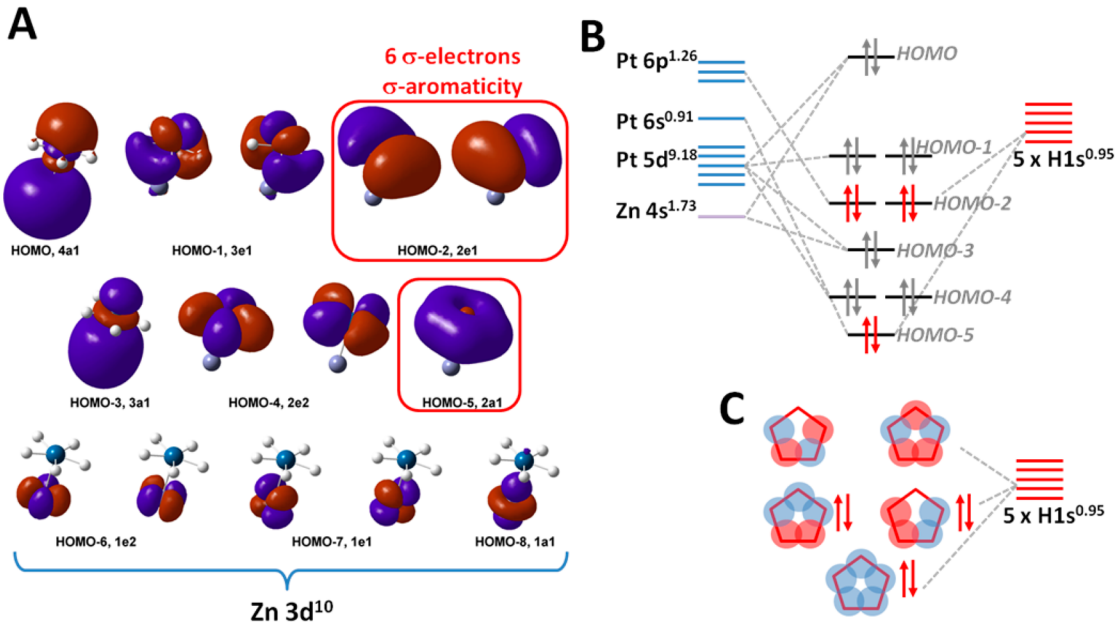

Figure 4. Chemical bonding in $PtZnH_5^-$. (A) Valence MOs, with the ones outlined in red corresponding to the σ-aromatic unit. (B) Correlation diagram for the valence MOs; the MOs outlined in red in (A) are highlighted. (C) A qualitative scheme for the formation of σ-MOs from five 1s AOs on H atoms in a pentagonal arrangement; the three lowest-energy MOs are analogous to those populated in the cluster; their population makes the cluster obey the $(4n + 2)$ Hückel's rule for aromatic compounds, with $n = 1$.

change upon relaxation, hence resulting in a small difference between the VDE and ADE.

Aromaticity of $PtZnH_5^-$. Figure 4 addresses the chemical bonding in the C_{5v} ($^1A_1$) isomer I of $PtZnH_5^-$. First of all, its structure is highly unusual due to its high symmetry and an anomalous coordination of the Pt atom, pentagonal pyramidal. Pt is often found to be square planar, but here, we have a five-coordinated arrangement in-plane and an additional Zn atom on the axial position. To the best of our knowledge, such coordination for Pt was never observed before. What leads to the stabilization of this unusual structure and the high abundance of this species in the mass spectrum of PtZn hydride anions? Valence MOs of the cluster are shown in Figure 4A, and a sketch of how they are formed from AOs is presented in Figure 4B. Some of the MOs of the cluster are clearly pure d lone pairs of Pt (HOMO−1 and HOMO−4) and Zn (HOMO−6, HOMO−7, and HOMO−8) that do not contribute to the bonding in the cluster. The HOMO and HOMO−3 correspond to σ-bonding between Pt and Zn. These MOs are mainly the bonding and antibonding combinations of the 4s AO on Zn and $5d_z^2$ AO on Pt. The Pt−Zn bond is partially ionic, with the partial charges on atoms being +0.011 on Zn and −1.355 on Pt (natural population analysis[31]). Importantly, removal of Zn from the cluster results in the PtH_5^- species, which is a planar D_{5h} structure (at least in the local minimum form), and the bonding within this fragment is analogous to that in the PtH_5^- unit within the $PtZnH_5^-$ hydride. Thus, Zn is merely a spectator in the system where Pt exhibits an unusual coordination.

The most interesting MOs are the doubly degenerate HOMO−2 and the HOMO−5 (Figure 4A). These are σ-MOs, mostly formed by the five 1s AOs on hydrides. They mix with the 6p and 6s AOs on Pt, as allowed by symmetry (Figure 4B). For simplicity, first consider just the isolated (hypothetic) H_5 pentagon. The five 1s AOs would form five MOs that are shown schematically in Figure 4C. The three lowest-energy ones correspond nicely to the valence HOMO−2 and HOMO−5 of $PtZnH_5^-$ in terms of contributions from

dx.doi.org/10.1021/jz500322n | J. Phys. Chem. Lett. 2014, 5, 1596−1601

hydrides. Hence, they are depicted populated in the scheme in Figure 4C. Populated by six electrons, the HOMO−2 and HOMO−5 make the cluster σ-aromatic,[11,32] in accord with the $(4n + 2)$ Hückel's electron counting rule for aromatic compounds with $n = 1$. Remarkably, σ-aromaticity was predicted for the isolated H_5^- (D_{5h}) cluster, but it was found to be a saddle point on the potential energy surface.[33] With the additional support of the 6s and 6p AOs on Pt, the aromatic all-H cycle is stabilized in the studied hydride. Pt is capable of sustaining the five-fold coordination in-plane because it is not really a five-fold coordination; it is a coordination to the H_5 pentagon (the complex can be described as $[Zn-Pt(\eta_5\text{-}H_5)]^-$), and the bonding within this unit is delocalized. Notably, transition metals can coordinate to five-membered ring structures, for example, in metallocenes, but there, the coordination is not in one plane. In $PtZnH_5^-$, Pt takes the central position in the ring to match the σ-MOs on H_5.

Besides the electron counting rule, we wished to gain an additional confirmation of aromaticity in this hydride. The calculation of the nucleus-independent chemical shifts (NICS)[34] index at the center of the pentagonal aromatic unit produces meaningless results because the geometric center coincides with the Pt atom and the contribution of the aromatic ring to the chemical shift is convoluted by the contributions from the AOs on Pt. We also applied the AdNDP[35] procedure, allowing for the maximal electron localization while preserving the electron pair paradigm. Two possible bonding pictures emerged from this analysis. One of them describes the H_5 arrangement σ-aromatic, with three localized AdNDP orbitals that look nearly identical to the HOMO−2 and HOMO−5 in Figure 4A. The contributions from Pt in this case were separated out to be lone pairs with fairly low population numbers of ∼1.6 e. The alternative picture produced five 2c−2e Pt−H bonds with population numbers of ∼1.9 e. Both pictures are valid from the AdNDP standpoint, and it is possible that there is a resonance between the two localized solutions. However, the presence of five covalent bonds in the plane mismatches the mutual orientations of the lobes of the AOs on Pt, making the picture counterintuitive. On the other hand, if one assumes the complete population of the 5d set and the 6s AOs and their overall spherical symmetry, then the H and Zn atoms would form an octahedral arrangement around Pt, not the pentagonal pyramidal arrangement. Thus, the five covalent bonds AdNDP picture is confusing. We therefore prefer the σ-aromaticity view of the studied hydride.

Aromaticity is a highly stabilizing effect, also responsible for high symmetry of the system. Therefore, we attribute the high abundance of the studied cluster in the mass spectrum and the apparent stability to σ-aromaticity. Our observation of the σ-aromatic arrangement of hydrides bound to metal clusters is important for catalysis applications. One may imagine that a cluster capable of hosting multiple H atoms that hold just the right charge may exhibit aromaticity and thus be unusually stable on the reaction profiles of the catalyzed reaction of dehydrogenation. This, however, remains to be demonstrated.

EXPERIMENTAL METHODS

The present work utilized negative ion PES as its primary probe. Anion PES is conducted by crossing a mass-selected beam of negative ions with a fixed-energy photon beam and energy analyzing the resulting photodetached electrons. This technique is governed by the energy-conservation relationship, $h\nu$ = EBE + EKE, where $h\nu$, EBE, and EKE are the photon energy, electron binding (transition) energy, and the electron kinetic energy, respectively. Our photoelectron spectrometer, which has been described in ref 30, consists of one of several ion sources, a linear time-of-flight mass spectrometer, a mass gate, a momentum decelerator, a neodymium-doped yttrium aluminum garnet (Nd:YAG) laser for photodetachment, and a magnetic bottle electron energy analyzer having a resolution of 35 meV at EKE = 1 eV. Photoelectron spectra were calibrated against the well-known photoelectron spectrum of Cu^-.[36] The $PtZnH_5^-$ anions were generated using a pulsed arc cluster ionization source (PACIS), which has been described in detail elsewhere.[37] In brief, a ∼30 μs long 150 V electrical pulse applied across the anode and sample cathode of the discharging chamber vaporizes the Pt and Zn atoms. The sample cathode was prepared in a nitrogen-protected glovebox, where fresh Zn and Pt powders were mixed and firmly pressed onto a zinc rod. Almost simultaneously, 250 psi of ultrahigh purity hydrogen gas was injected into the discharge region, where it was dissociated into hydrogen atoms. The resulting mixture of atoms, ions, and electrons then reacted and cooled as it flowed along a 20 cm tube before exiting into high vacuum. The resulting anions were then extracted and mass-selected prior to photodetachment. The $PtZnH_5^-$ cluster anion has several isotopes; therefore, photoelectron spectra were taken from all of the isotopic peaks to confirm that there were no impurities in the mass spectrum.

COMPUTATIONAL METHODS

The search for the global minima of the studied cluster anions was done using the gradient embedded genetic algorithm (GEGA),[38] with the population size of 20, and the UPBEPBE[39]/LANL2DZ[40] method. Separate searches for several spin states were performed. The lowest-energy isomers were characterized at higher levels of theory, UPBEPBE/aug-cc-pvTZ+pp,[41] UM06,[42] single-point CCSD[43]//UPBE, and CASSCF(m,n),[44] with (m,n) being as large as (12,12), with the same basis set. It was found that the perturbation theory fails for the studied systems, and for this reason, MP-based methods and CCSD(T) were not used. The combination of Pople's 6-311++G**[45] basis for Zn and H and the LANL2DZ basis for Pt were also used to make sure that there is no unhealthy dependence on the choice for the basis set. For calculations of photoelectron spectra, linear response time-dependent DFT, TD-UPBEPBE, with different basis sets, and also CCSD/aug-cc-pvTZ+pp//UPBEPBE/aug-cc-pvTZ+pp were used. TD-DFT was used for calculations of the excited states of the neutral clusters, and then, the excitation energies were added to the value of the first vertical detachment energy (VDE_1) to produce VDE_2, VDE_3, and so forth. All calculations were done with Gaussian 09.[46]

ASSOCIATED CONTENT

Supporting Information

Calculated energy differences between isomers I and II and calculated properties of isomers I and II. This material is available free of charge via the Internet at http://pubs.acs.org.

AUTHOR INFORMATION

Corresponding Authors

*E-mail: kbowen@jhu.edu (K.H.B.).
*E-mail: ana@chem.ucla.edu (A.N.A.).

Notes

The authors declare no competing financial interest.

dx.doi.org/10.1021/jz500322n | J. Phys. Chem. Lett. 2014, 5, 1596−1601

■ ACKNOWLEDGMENTS

This material is based in part on work supported by the Air Force Office of Scientific Research (AFOSR) under Grant Numbers FA9550-11-1-0068 (K.H.B.) and 10029173-S3 (A.N.A.). A.N.A. also thanks the Alfred P. Sloan Foundation Fellowship. The AdNDP calculation was performed by Timur Galeev. We thank Alexander Boldyrev for useful discussion.

■ REFERENCES

(1) Li, X.; Kuznetsov, A. E.; Zhang, H. F.; Boldyrev, A. I.; Wang, L. S. Observation of All-Metal Aromatic Molecules. *Science* **2001**, *291*, 859−861.

(2) Li, X.; Zhang, H. F.; Wang, L. S.; Kuznetsov, A. E.; Cannon, N. A.; Boldyrev, A. I. Experimental and Theoretical Observations of Aromaticity in Heterocyclic XAl_3^- (X = Si, Ge, Sn, Pb) Systems. *Angew. Chem., Int. Ed.* **2001**, *113*, 1919−1922.

(3) Kuznetsov, A. E.; Boldyrev, A. I.; Li, X.; Wang, L. S. On the Aromaticity of Square Planar Ga_4^{2-} and In_4^{2-} in Gaseous $NaGa^{4-}$ and $NaIn^{4-}$ Clusters. *J. Am. Chem. Soc.* **2001**, *123*, 8825−8831.

(4) Boldyrev, A. I.; Kuznetsov, A. E. On the Resonance Energy in New All-Metal Aromatic Molecules. *Inorg. Chem.* **2002**, *41*, 532−537.

(5) Kuznetsov, A. E.; Boldyrev, A. I.; Zhai, H. J.; Li, X.; Wang, L. S. Al_6^{2-} Fusion of Two Aromatic Al_3^- Units. A Combined Photoelectron Spectroscopy and Ab Initio Study of M^+ $[Al_6^{2-}]$ (M = Li, Na, K, Cu, and Au). *J. Am. Chem. Soc.* **2002**, *124*, 11791−11801.

(6) Kuznetsov, A. E.; Boldyrev, A. I. Theoretical Evidence of Aromaticity in X_3^- (X = B, Al, Ga) Species. *Struct. Chem.* **2002**, *13*, 141−148.

(7) Alexandrova, A. N.; Boldyrev, A. I. σ-Aromaticity and σ-Antiaromaticity in Alkali Metal and Alkaline Earth Metal Small Clusters. *J. Phys. Chem. A* **2003**, *107*, 554−560.

(8) Tanaka, H.; Neukermans, S.; Janssens, E.; Silverrans, R. E.; Lievens, P. σ-Aromaticity of the Bimetallic Au_5Zn^+ Cluster. *J. Am. Chem. Soc.* **2003**, *125*, 2862−2863.

(9) Boldyrev, A. I.; Wang, L. S. All-Metal Aromaticity and Antiaromaticity. *Chem. Rev.* **2005**, *105*, 3716−3757.

(10) Alexandrova, A. N. Tug of War Between AO-Hybridization and Aromaticity in Dictating Structures of Li-Doped Alkali Clusters. *Chem. Phys. Lett.* **2012**, *533*, 1−5.

(11) Alexandrova, A. N.; Boldyrev, A. I.; Li, X.; Sarkas, H. W.; Hendricks, J. H.; Arnold, S. T.; Bowen, K. H. Lithium Cluster Anions: Photoelectron Spectroscopy and Ab Initio Calculations. *J. Chem. Phys.* **2011**, *134*, 044322/1−044322/8.

(12) Li, Z. H.; Moran, D.; Fan, K. N.; Schleyer, P. v. R. σ-Aromaticity and σ-Antiaromaticity in Saturated Inorganic Rings. *J. Phys. Chem. A* **2005**, *109*, 3711−3716.

(13) Zhang, J.; Alexandrova, A. N. Double σ-Aromaticity in a Surface-Deposited Cluster: Pd_4 on TiO_2(110). *J. Phys. Chem. Lett.* **2012**, *3*, 751−754.

(14) Zubarev, D. Y.; Averkiev, B. B.; Zhai, H. J.; Wang, L. S.; Boldyrev, A. I. Aromaticity and Antiaromaticity in Transition-Metal Systems. *Phys. Chem. Chem. Phys.* **2008**, *10*, 257−267.

(15) Galeev, T. R.; Boldyrev, A. I. Recent Advances in Aromaticity and Antiaromaticity in Transition-Metal Systems. *Annu. Rep. Prog. Chem., Sect. C* **2001**, *107*, 124−147.

(16) Kuznetsov, A. E.; Birch, K. A.; Boldyrev, A. I.; Li, X.; Zhai, H. J.; Wang, L. S. All-Metal Antiaromatic Molecule: Rectangular Al_4^{4-} in the $Li_3Al_4^-$ Anion. *Science* **2003**, *300*, 622−625.

(17) Tsipis, A. C.; Tsipis, C. A. Hydrometal Analogues of Aromatic Aydrocarbons: a New Class of Cyclic Hydrocoppers (I). *J. Am. Chem. Soc.* **2003**, *125*, 1136−1137.

(18) Tsipis, C. A.; Karagiannis, E. E.; Kladou, P. F.; Tsipis, A. C. Aromatic Gold and Silver Rings: Hydrosilver (I) and Hydrogold (I) Analogues of Aromatic Hydrocarbons. *J. Am. Chem. Soc.* **2004**, *126*, 12916−12929.

(19) Tsipis, A. C.; Tsipis, C. A. Ligand-Stabilized Aromatic Three-Membered Gold Rings and their Sandwich-Like Complexes. *J. Am. Chem. Soc.* **2005**, *127*, 10623−10638.

(20) Tsipis, A. C.; Stalikas, A. V. A New Alass of "All-Metal" Aromatic Hydrido-Bridged Binary Coinage Metal Heterocycles. A DFT Study. *New J. Chem.* **2007**, *31*, 852−859.

(21) Kang, Y. J.; Pyo, J. B.; Ye, X. C.; Gordon, T. R.; Murray, C. B. Synthesis, Shape Control, and Methanol Electro-oxidation Properties of Pt−Zn Alloy and Pt_3Zn Intermetallic Nanocrystals. *ACS Nano* **2012**, *6*, 5642−5647.

(22) Miura, A.; Wang, H.; Leonard, B. M.; Abruna, H. D.; DiSalvo, F. J. Synthesis of Intermetallic PtZn Nanoparticles by Reaction of Pt Nanoparticles with Zn Vapor and Their Application as Fuel Cell Catalysts. *Chem. Mater.* **2009**, *21*, 2661−2667.

(23) Galloway, E.; Armbrüster, M.; Kovnir, K.; Tikhov, M. S.; Lambert, R. M. Bromine-Promoted PtZn is Very Effective for the Chemoselective Hydrogenation of Crotonaldehyde. *J. Catal.* **2009**, *261*, 60−65.

(24) Rossmeisl, J.; Karlberg, G. S.; Jaramillo, T.; Norskov, J. K. Steady State Oxygen Reduction and Cyclic Voltammetry. *Faraday Discuss.* **2009**, *140*, 337−346.

(25) Martono, E.; Vohs, J. M. Reaction of CO, CH_2O, CH_3OH on Zn-Modified Pt (111) Surfaces. *J. Phys. Chem. C* **2013**, *117*, 6692−6701.

(26) McManus, J. R.; Martono, E.; Vohs, J. M. Selective Deoxygenation of Aldehydes: The Reaction of Acetaldehyde and Glycolaldehyde on Zn/Pt (111) Bimetallic Surfaces. *ACS Catal.* **2013**, *3*, 1739−1750.

(27) Lee, S.; Fan, C.; Wu, T.; Anderson, S. L. CO Oxidation on Au_n/TiO_2 Catalysts Produced by Size-Selected Cluster Deposition. *J. Am. Chem. Soc.* **2004**, *126*, 5682−5683.

(28) Fu, Q.; Saltsburg, H.; Flytzani-Stephanopoulos, M. Active Nonmetallic Au and Pt Species on Ceria-Based Water−Gas Shift Catalysts. *Science* **2003**, *301*, 935−938.

(29) Herzing, A. A.; Kiely, C. J.; Carley, A. F.; Landon, P.; Hutchings, G. J. Identification of Active Gold Nanoclusters on Iron Oxide Supports for CO Oxidation. *Science* **2008**, *321*, 1331−1335.

(30) Gerhards, M.; Thomas, O. C.; Nilles, J. M.; Zheng, W. L.; Bowen, K. H. Cobalt−Benzene Cluster Anions: Mass Spectrometry and Negative Ion Photoelectron Spectroscopy. *J. Chem. Phys.* **2002**, *116*, 10247−10252.

(31) (a) Carpenter, J. E.; Weinhold, F. Analysis of the Geometry of the Hydroxymethyl Radical by the "Different Hybrids for Different Spins" Natural Bond Orbital Procedure. *J. Mol. Struct.: THEOCHEM* **1988**, *169*, 41−62. (b) Carpenter, J. E. Ph.D. Thesis, University of Wisconsin, Madison, WI, 1987. (c) Foster, J. P.; Weinhold, F. Natural Hybrid Orbitals. *J. Am. Chem. Soc.* **1980**, *102*, 7211−7218. (d) Reed, A. E.; Weinhold, F. Natural Bond Orbital Analysis of Near-Hartree−Fock Water Dimer. *J. Chem. Phys.* **1983**, *78*, 4066−4073. (e) Reed, A. E.; Curtiss, L. A.; Weinhold, F. Intermolecular Interactions from a Natural Bond Orbital, Donor−Acceptor Viewpoint. *Chem. Rev.* **1988**, *88*, 899−926.

(32) (a) Alexandrova, A. N.; Boldyrev, A. I. s-Aromaticity and s-Antiaromaticiy in Alkaline Metal and Alkaline Earth Metal Small Clusters. *J. Phys. Chem. A* **2003**, *107*, 554−560.

(33) Jiao, H.; Schleyer, P. v. R.; Glukhovtsev, M. N. Are the D_{mh} Symmetric H_x^q Rings with $4n + 2$ s-Electrons and Hydrogen Clusters Aromatic? *J. Phys. Chem.* **1996**, *100*, 12299−12304.

(34) Schleyer, P. V. R.; Maerker, C.; Dransfeld, A.; Jiao, H.; Hommes, N. E. R. v. E. Nucleus-Independent Chemical Shifts (NICS): A Simple and Efficient Aromaticity Probe. *J. Am. Chem. Soc.* **1996**, *118*, 6317−6318.

(35) Zubarev, D. Yu.; Boldyrev, A. I. Developing Paradigms of Chemical Bonding: Adaptive Natural Density Partitioning. *Phys. Chem. Chem. Phys.* **2008**, *10*, 5207−5217.

(36) Ho, J.; Ervin, K. M.; Lineberger, W. C. Photoelectron Spectroscopy of Metal Cluster Anions: Cu, Ag, and Au. *J. Chem. Phys.* **1990**, *93*, 6987.

(37) Li, X.; Grubisic, A.; Stokes, S. T.; Cordes, J.; Gantefoer, G. F.; Bowen, K. H.; Kiran, B.; Willis, M.; Jena, P.; Burgert, R.; Schnoeckel, H. Unexpected Stability of Al_4H_6: A Borane Analog? *Science* **2007**, *315*, 356−358.

(38) (a) Alexandrova, A. N. $H\cdot(H_2O)_n$ Clusters: Microsolvation of the Hydrogen Atom via Molecular Ab Initio Gradient Embedded Genetic Algorithm (GEGA). *J. Phys. Chem. A* **2010**, *114*, 12591−12599. (b) Alexandrova, A. N.; Boldyrev, A. I. Theory Comput. Search for the $Li_x^{0/+1/-1}$ Lowest Energy Structuresc Using Ab Initio Gradient Embedded Genetic Algorithm (GEGA). Elucidation of the Chemical Bonding in the Lithium Clusters. *J. Chem. Theory. Comput.* **2005**, *1*, 566−580. (c) Alexandrova, A. N.; Boldyrev, A. I.; Fu, T. J.; Yang, X.; Wang, X. B.; Wang, L. S. structure of the $Na_xCl_{x+1}^-$ (x=1−4) Clusters via Ab Initio Genetic Algorithm and Photoelectron Spectroscopy. *J. Chem. Phys.* **2004**, *121*, 5709.

(39) Perdew, J. P.; Burke, K.; Ernzerhof, M. Generalized Gradient Approximation Made Simple. *Phys. Rev. Lett.* **1996**, *77*, 3865−3868.

(40) (a) Hay, P. J.; Wadt, W. R. Ab Initio Effective Core Potentials for Molecular Calculations. Potentials for the Transition Metal Atoms Sc to Hg. *J. Chem. Phys.* **1985**, *82*, 270. (b) Hay, P. J.; Wadt, W. R. Ab Initio Effective Core Potentials for Molecular Calculations. Potentials for Main Group Elements Na to Bi. *J. Chem. Phys.* **1985**, *82*, 284. (c) Hay, P. J.; Wadt, W. R. Ab Initio Effective Core Potentials for Molecular Calculations. Potentials for K to Au Including the Outermost Core Orbitals. *J. Chem. Phys.* **1985**, *82*, 299.

(41) Peterson, K. A.; Puzzarini, C. Systematically Convergent Basis Sets for Transition Metals. II. Pseudopotential-Based Correlation Consistent Basis Sets for the Group 11 (Cu, Ag, Au) and 12 (Zn, Cd, Hg) Elements. *Theor. Chem. Acc.* **2005**, *114*, 283−296.

(42) Zhao, Y.; Truhlar, D. G. The M06 Suite of Density Functionals for Main Group Thermochemistry, Thermochemical Kinetics, Noncovalent Interactions, Excited States, and Transition Elements: Two New Functionals and Systematic Testing of Four M06-Class Functionals and 12 Other Functionals. *Theor. Chem. Acc.* **2008**, *120*, 215−241.

(43) (a) Cizek, J. On the Use of the Cluster Expansion and the Technique of Diagrams in Calculations of Correlation Effects in Atoms and Molecules. *Adv. Chem. Phys.* **1969**, *14*, 35−89. (b) Purvis, G. D., III; Bartlett, R. L. A Full Coupled-Cluster Singles and Doubles Model: The Inclusion of Disconnected Triples. *J. Chem. Phys.* **1982**, *76*, 1910. (c) Scuseria, G. E.; Janssen, C. L.; Schaefer, H. F., III. An Efficient Reformulation of the Closed-Shell Coupled Cluster Single and Double Excitation (CCSD) Equations. *J. Chem. Phys.* **1988**, *89*, 7382. (d) Scuseria, G. E.; Schaefer, H. F., III. Is Coupled Cluster Singles and Doubles (CCSD) More Computationally Intensive than Quadratic Configuration Interaction (QCISD)? *J. Chem. Phys.* **1989**, *90*, 3700.

(44) (a) Pople, J. A.; Head-Gordon, M.; Raghavachari, K. J. A. Quadratic Configuration Interaction. A General Technique for Determining Electron Correlation Energies. *J. Chem. Phys.* **1987**, *87*, 5968. (b) Hegarty, D.; Robb, M. A. Application of Unitary Group Methods to Configuration Interaction Calculations. *Mol. Phys.* **1979**, *38*, 1795−1812. (c) Eade, R. H. A.; Robb, M. A. Direct Minimization in MC SCF Theory. The Quasi-Newton Method. *Chem. Phys. Lett.* **1981**, *83*, 362−368. (d) Bernardi, F.; Bottini, A.; McDougall, J. J. W.; Robb, M. A.; Schlegel, H. B. MCSCF Gradient Calculation of Transition Structures in Organic Reactions. *Faraday Symp. Chem. Soc.* **1984**, *19*, 137−147. (f) Frisch, M. J.; Ragazos, I. N.; Robb, M. A.; Schlegel, H. N. An Evaluation of Three Direct MC-SCF Procedures. *Chem. Phys. Lett.* **1992**, *189*, 524−528. (g) Yamamoto, N.; Vreven, T.; Robb, M. A.; Frisch, M. J.; Schlegel, H. B. A Direct Derivative MC-SCF Procedure. *Chem. Phys. Lett.* **1996**, *250*, 373−378.

(45) (a) Clark, T.; Chandrasekhar, J.; Spitznagel, C. W.; Schleyer, P. v. R. Efficient Diffuse Function-Augmented Basis Sets for Anion Calculations. III. The 3-21+G Basis Set for First-Row Elements, Li−F. *J. Comput. Chem.* **1983**, *4*, 294−301. (b) Frisch, M. J.; Pople, J. A.; Binkley, J. S. Self-Consistent Molecular Orbital Methods 25. Supplementary Functions for Gaussian Basis Sets. *J. Chem. Phys.* **1984**, *80*, 3265.

(46) Frisch, M. J.; Trucks, G. W.; Schlegel, H. B.; Scuseria, G. E.; Robb, M. A.; Cheeseman, J. R.; Scalmani, G.; Barone, V.; Mennucci, B.; Petersson, G. A.; et al. *Gaussian 09*, revision A.1; Gaussian, Inc.: Wallingford, CT, 2009.